Contract No:

This document was prepared in conjunction with work accomplished under Contract No. DE-AC09-08SR22470 with the U.S. Department of Energy (DOE) Office of Environmental Management (EM).

Disclaimer:

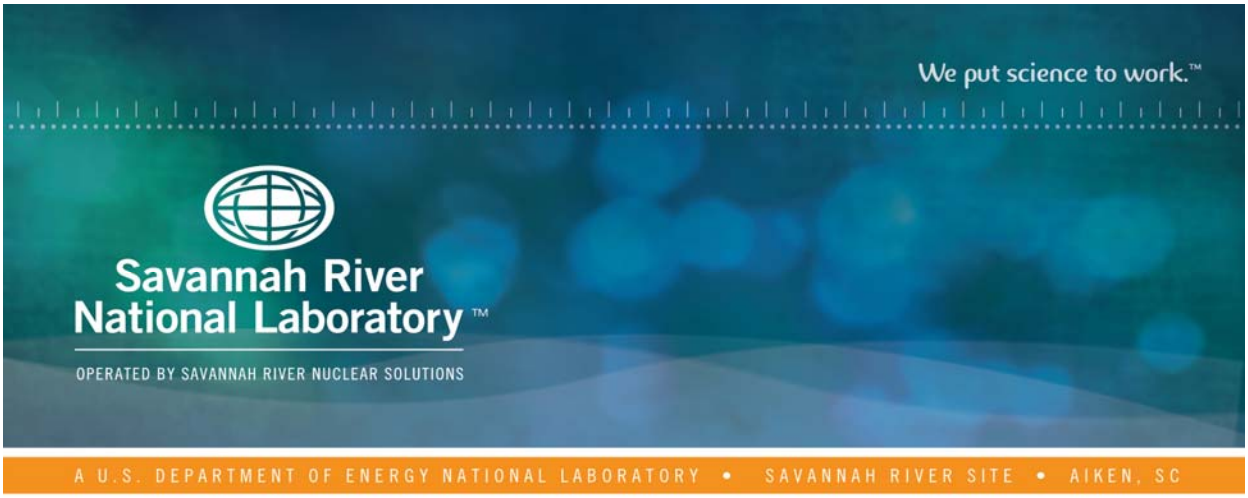

Preliminary Analysis of Species Partitioning in the DWPF Melter - Sludge Batch 7a

A. S. Choi
F. G. Smith, III
D. J. McCabe

January 2017
SRNL-STI-2016-00540, Revision 0

DISCLAIMER

Printed in the United States of America

Prepared for
U.S. Department of Energy

SRNL-STI-2016-00540
Revision 0

Keywords: *DWPF Melter, Off-Gas Entrainment, Technetium, HTWOS Model*

Retention: *Permanent*

Preliminary Analysis of Species Partitioning in the DWPF Melter - Sludge Batch 7a

A. S. Choi
F. G. Smith, III
D. J. McCabe

January 2017

Prepared for the U.S. Department of Energy under contract number DE-AC09-08SR22470.

Savannah River National Laboratory™
OPERATED BY SAVANNAH RIVER NUCLEAR SOLUTIONS

REVIEWS AND APPROVALS

AUTHORS:

Alexander S. Choi, Process Technology Programs/SRNL Date

Frank G. Smith, III, Radiological Performance Assessment/SRNL Date

Daniel J. McCabe, Hanford Mission Programs/SRNL Date

TECHNICAL REVIEW:

Alexander S. Choi, Reviewed All Sections per E7 2.60 Date

Frank G. Smith, III, Reviewed All Sections per E7 2.60 Date

Devon L. McClane, Engineering Process Development/SRNL Date

APPROVAL:

E. N. Hoffman, Manager Date
Engineering Process Development, E&CPT Research Programs/ES/SRNL

C. C. Herman, Director Date
Hanford Mission Programs/Environmental Stewardship (ES)/SRNL

D. E. Dooley, Director Date
Environmental & Chemical Process Technology (E&CPT) Research Programs/ES/SRNL

ACKNOWLEDGEMENT

This work was performed as part of the Technetium Management Program Plan by the U.S. Department of Energy (DOE), Office of Environmental Management. We would like to thank Dr. Nicholas Machara of the Office of Technology Development for his continuing support of this work. We would also like to thank Brandon Hodge, Jim Coleman and Jeremiah Ledbetter of Savannah River Remediation (SRR) for their continuing support in terms of providing the extensive DWPF operating data that formed the basis of this work and David McGuire of SRNL for interfacing with the SRR personnel for the necessary data collection. We would also like to recognize Fabienne Johnson of SRNL for compiling the analytical data for the Tank 40 sludge and glass pour stream samples in a spreadsheet for ready input into the model. Finally, we would like to thank all DOE and SRNL personnel who reviewed the draft report and provided insightful comments. Particularly, the extensive comments provided by Dr. A. Kruger of the Office of River Protection (ORP) at the DOE's Hanford Site helped improve the clarity and completeness of the technical contents presented in this report.

EXECUTIVE SUMMARY

The work described in this report is preliminary in nature since its goal was to demonstrate the feasibility of estimating the off-gas carryover from the Defense Waste Processing Facility (DWPF) melter based on a simple mass balance using measured feed and glass pour stream (PS) compositions and time-averaged melter operating data over the duration of one canister-filling cycle. The method was tested earlier against the Sludge Batch 6 (SB6) PS sample data taken while Canister #3472 was being filled over a 20-hour period on 12/20/2010, approximately three months after the glass bubblers were installed. The analytical results for that PS sample provided the necessary glass composition for the mass balance calculations. To estimate the "matching" feed composition, which is not necessarily the same as that of the Melter Feed Tank (MFT) batch being fed at the time of PS sampling, a mixing model was developed involving three preceding MFT batches as well as that being fed at that time of PS sampling. The model assumes perfect mixing in the melt pool but with an induction period to account for the process delays involved in the calcination and fusion reactions in the cold cap and thus reduced the number of melter turnover for the last batch. The results of the SB6 mass balance showed that the proposed method of estimating the off-gas carryover or entrainment rate from measured feed and PS compositions appears feasible at least for the major species (e.g., Si, Na, Fe and Al) and thus additional case studies were recommended (SRNL-STI-2015-00279).

The DWPF has been in radioactive operation for over 20 years processing a wide range of high-level waste (HLW) feed compositions under varying conditions such as bubbled vs. non-bubbled and feeding vs. idling. So it is desirable to find out how the varying feed compositions and operating parameters would have impacted the off-gas entrainment. However, the DWPF melter is not equipped with off-gas sampling or monitoring capabilities, so it is not feasible to measure off-gas entrainment rates directly. The proposed method provides an indirect way of doing so; it is a series of calculation steps used to extract off-gas entrainment information from available feed and PS sample characterization and melter operating data. This method was tested further in this study using the SB7a PS sample data taken while Canister #3619 was being filled over a 21-hour period on 8/5/2011 with the glass bubblers in operation. In doing so, several changes were made to the approach used in the SB6 analysis in an effort to more accurately interpret and apply the available DWPF operating data. First, the total number of MFT batches considered in the melt pool mixing model was increased from 4 to 5, including that fed at the time of PS sampling. Second, dilution of feed by the addition of trickle water flow into the MFT and subsequent decreases in total solids and density over the course of each batch processing were accounted for. Third, the blending of waste and frit in the Slurry Mix Evaporator (SME) was modeled at the ratio reported in the Product Composition Control System (PCCS) spreadsheet as part of the acceptability testing of each SME batch. Fourth, the measured slurry feed rate to the melter in gal/min (GPM), which is known to be higher than that estimated based on the MFT level data by up to 15%, was adjusted down by 7.5%. The results of the SB7a mass balance showed that:

- The overall calculated entrainment rate of the bubbled DWPF melter was high at 3.7% of the SB7a calcined solids fed vs. 2.4% calculated earlier for the SB6. By comparison, the design basis entrainment rate from non-bubbled DWPF melter is 1%. However, the actual overall entrainment rate of the SB7a is likely to be lower than 3.7% due to potential under measurement of Al and Na concentrations in the pour stream sample.

- The average entrainment rate of the four major non-volatile sludge components (Al, Fe, Mn and U) was calculated to be 2.4% of the amount fed, which appears to be statistically the same as 2.7% calculated for the SB6. However, the estimated entrainment rate for SB7a was skewed since it includes high entrainment rates of 8.8% and 2.2% for Al and Fe, respectively, and the negative entrainment rate of -1.5% for U.

- The average entrainment rate of the frit components, excluding Na, was lower than the non-volatile sludge components at 0.8% fed, which also appears to be statistically the same as 0.7% calculated for the SB6. The entrainment rate of Na was high at 14.2% fed vs. 7.5% for the SB6.

- The entrainment rate of Cs-137 was calculated to be 13.6% of the amount fed vs. 16.4% for SB6.

- The entrainment rate of Tc-99 was calculated to be high but approximately less than 60% of the amount fed. The corresponding entrainment rate of SB6 could not be calculated as the concentration of Tc-99 in Tank 40 and PS sample was both below the detection limit.

- The measured REDOX of the SB7a PS sample was 0.13, while that of the MFT Batch 580 sample was 0.04 in a closed crucible. The higher REDOX of the SB7a PS sample (than that of the closed crucible sample measured in the laboratory) was expected as the argon bubbling of the melt pool is known to make glass more reducing.

- The total processing time for the 5 MFT batches considered in this study was 540 hours, and the melter remained idling for 19 hours (3.4% of the time) vs. 250 hours of idling out of 602 hours total (41.5% of the time) for the SB6. As expected, the longer idling during SB6 appears to have contributed to a greater loss of volatile species such as Cs, as noted above.

- The estimated DWPF entrainment rates were in general higher than those measured during the DM1200 runs at the Vitreous State Laboratory (VSL) using the Hanford HLW AZ-101 simulants. This may be attributed in part to the formic acid used as the reductant for the DWPF feeds (compared to sugar used for the DM1200 feed) as well as the higher glass bubbling flux used in the DWPF melter.

The uncertainty analysis of the results highlighted above was not performed in this study for two reasons. First, although this method calculates the entrainment rates of individual components as the difference between their feed and pour rates, which sounds simple, it requires both analytical and plant operating data taken under steady state conditions and the uncertainty bounds of the latter are difficult to determine. Second, a true steady state operation is seldom achieved, if at all possible, in an actual production melter environment. For example, glass is not poured into a canister at a uniform rate and, to overcome this, the average pour rate is calculated based on the total glass poured and the time it takes to fill each canister. However, if there is a net change in melt level before and after the pouring operation, the calculated pour rate needs to be adjusted accordingly to preserve the steady state assumption, including a constant melt level. As stated above, the interpretation and application of the plant operating data have been made more relevant in this study in consultation with the DWPF personnel and additional work is clearly needed to eventually determine the uncertainty bounds of some of the key operating data, including the measured slurry feed rate. Until then, the results presented in this report should be taken as "preliminary."

The path forward is to continue testing of the proposed method for additional sludge batches, provided relevant analytical and operating data is retrievable. The resulting database of calculated entrainment rates will then be screened in terms of bubbling flux, percent idling time, REDOX, melt viscosity, vapor space height, etc. Once key design and operating variables are gleaned from DWPF data, a regression analysis coupled with the high-temperature thermodynamic modeling of calcination and fusion reactions will be performed on the entire entrainment database, both calculated for the DWPF melter and measured during non-DWPF melter runs. The ultimate goal of this task is to develop a correlation for predicting off-gas entrainment rates from both the Low Activity Waste (LAW) and HLW melters of the Waste Treatment Plant (WTP) as a function of key operating parameters and incorporate it into the TOPsim model as well as the dynamic flowsheet model based on Gensym's G2® programming language.

TABLE OF CONTENTS

LIST OF TABLES

LIST OF FIGURES

LIST OF ACRONYMNS

AR	Aqua Regia
ARP	Actinide Removal Process
CSSX	Caustic-Side Solvent Extraction
DCS	Distributed Control System
DF	Decontamination Factor
DOE	Department of Energy
DWPF	Defense Waste Processing Facility
GPCP	Glass Product Control Program
GPM	Gallons per Minute
HLW	High-Level Waste
HTWOS	Hanford Tank Waste Operations Simulator
LSFM	Large-Slurry Fed Melter
LAW	Low-Activity Waste
MCU	Modular CSSX Unit
MFT	Melter Feed Tank
ORP	Office of River Protection
PCCS	Product Composition Control System
PF	Peroxide Fusion
PS	Pour Stream
REDOX	REDuction-OXidation
SB	Sludge Batch
SBS	Submerged Bed Scrubber
SME	Slurry Mix Evaporator
SRAT	Sludge Receipt and Adjustment Tank
SRNL	Savannah River National Laboratory
SRS	Savannah River Site
TIC	Total Inorganic Carbon
TOC	Total Organic Carbon
TSR	Technical Safety Requirement
VSL	Vitreous State Laboratory
WL	Waste loading
WTP	Waste Treatment Plant

1.0 Introduction

As part of the overall effort to support the technetium (Tc) management project at the Hanford Site,[1] this task seeks to develop an improved capability for predicting the partitioning of species in the Low Activity Waste (LAW) melter between the glass and off-gas entrainment for integration into the Hanford Tank Waste Operations Simulator (HTWOS) flowsheet model.[2] This approach will also be applicable to the HLW melter. (Note the software platform for the HTWOS model has since changed and the new model is now called TOPsim.) Specifically, it is desirable to know what fraction of the key radioactive and non-radioactive species fed to the melter would be entrained into the off-gas and their subsequent fates in the off-gas condensate collection and treatment system. A staged approach to achieving this goal is outlined in the task plan;[2] (1) understanding of the TOPsim model construct, (2) data mining on off-gas carryover or entrainment rates preferentially from large-scale melters, (3) empirical modeling of the overall off-gas entrainment rates, (4) thermodynamic modeling of the vitrification process to estimate entrainment rates due to vapor-pressure-driven transport, (5) aqueous electrolyte modeling of off-gas condensate chemistry, and (6) integration of species partitioning algorithms into the TOPsim and G2® flowsheet models.

The melter feed and glassy materials can enter the off-gas system in two ways. First, they can become airborne by a sudden surge of steam and calcine gases ejecting out of the cold cap. This physical mode of entrainment is influenced by not only the melter design and operating variables such as glass bubbling rate but the feed chemistry and rheology as well. The other mode of entrainment is chemical in nature; some species such as CsCl becomes volatile at the nominal glass temperature of 1,150 °C and exit the melter as vapor only to condense into an aerosol when it cools downstream of the melter. Under normal feeding/pouring operation, particulate carryover is dominated by the physical entrainment. Under idling mode, however, particulate carryover decreases dramatically since it occurs by volatility alone. Off-gas entrainment data is typically reported as the sum of both physical and vapor-pressure-driven entrainments.

Stages 1 and 2 of the task plan listed above were completed in 2014. Specifically, the off-gas entrainment data collected during Stage 2 came from two sources; (1) DM1200 melter runs at the Vitreous State Laboratory (VSL) using both the High-Level Waste (HLW) and Low-Activity Waste (LAW) simulants for the Waste Treatment Plant (WTP) blended with glass-forming chemicals,[3] and (2) the Large Slurry-Fed Melter (LSFM) runs at the Savannah River National Laboratory (SRNL) using various DWPF feed simulants coupled with glass-forming frits.[4] (Note that only one representative reference is given here for each melter run as an example instead of citing all the reports from which entrainment data was obtained.) Both DM1200 and LSFM were targeted since they are relatively large in scale, each having a melt surface area equaling 42 to 45% of the Defense Waste Processing Facility (DWPF) melter at the Savannah River Site (SRS). The methods of off-gas sampling and analysis used in the two melter runs were also similar; the off-gas was sampled isokinetically downstream of the film cooler and the particulate collected was characterized and quantified for the elemental mass balance. The entrainment rates were measured under different operating conditions by varying the bubbling rate and/or number of bubblers, feed chemistry, etc., and the data thus collected will form part of the basis for the empirical modeling in Stage 3.

The feasibility of expanding the range of data collected in Stage 2 was assessed in an earlier study by including the DWPF melter data taken in a radioactive production environment during the processing of Sludge Batch 6 (SB6).[5] The scope of the available DWPF data is broad but, as is the case with most manufacturing plants, data collection is geared toward production support through process control and troubleshooting. For example, the DWPF melter is equipped with comprehensive pressure, temperature, and flow control loops but has no off-gas sampling or monitoring capabilities, which means that off-gas entrainment rates cannot be measured directly. Samples of off-gas deposits and condensate have been taken and analyzed since the radioactive startup in 1996 but, since they were not collected in any controlled manner, necessary quantitative information for the estimation of species partitioning between

the glass and off-gas entrainment could not be obtained. So the remaining option is indirect estimation based on the component mass balance using measured feed and glass compositions. Specifically, during each sludge batch campaign, the DWPF is required to take at least one glass sample to meet the objectives of the Glass Product Control Program (GPCP) and complete the necessary Production Records so that the final glass product may be disposed of at a Federal Repository yet to be determined.[6] Each sludge batch campaign lasts long enough to produce on average ~500 glass canisters, each containing ~4,000 lb of glass. Thus, it was proposed that steady state mass balance be set up around the time of glass pour stream (PS) sampling and off-gas entrainment rates be calculated as the difference between the calcined feed and glass pour rates as a representation for the entire sludge batch.[5]

This proposed method was tested earlier using the SB6 PS sample taken while Canister #3472 was being filled over a 20-hour period on 12/20/2010, approximately three months after the glass bubblers were installed.[5] The analytical results for that PS sample provided the necessary glass composition for the mass balance calculations. To estimate the "matching" feed composition, which is not necessarily the same as that of the Melter Feed Tank (MFT) batch being fed at the time of PS sampling, a mixing model was developed by including three preceding MFT batches as well assuming perfect mixing in the melt pool. The melter turnover achieved while feeding the last batch up to the time of PS sampling was reduced by; (1) introducing a 2-hr induction period to account for the process delays associated with the calcination and fusion of feed solids in the cold cap and (2) subtracting the glass residence time of on the order of 50-60 hours to account for the mixing delay. Comparison of the resulting SB6 entrainment ratios with the DWPF design basis values and those measured during the DM1200 run showed that the proposed method of estimating off-gas carryover from a simple mass balance appears feasible at least for the major species (e.g., Si, Na, Fe and Al) and thus additional case studies were recommended.[5]

Testing of the proposed method continued in this study using the SB7a PS sample data taken while Canister #3619 was being filled over a 21-hour period on 8/5/2011 with the glass bubblers in operation. Several changes were made to the approach used in the SB6 mass balance in an effort to more accurately interpret and apply available operating/process data, including dilution of each MFT batch by the addition of trickle water flow, blending of waste and frit according to the ratios reported in the Product Composition Control System (PCCS) spreadsheet and adjustment of measured slurry feed rates to the melter. This report documents these changes in detail and compares the resulting entrainment ratios of the SB7a to those of the SB6 as well as the DM1200.

2.0 DWPF Flowsheet

Figure 1 shows a simplified flow diagram of the processing units, including the melter, which provides the bulk of the necessary process/operating data for this work. Tank 40 is a staging tank with over one-million gallon capacity where each washed sludge batch is stored. The composition of Tank 40 content is fully characterized, including a complete radioisotope analysis, as part of the sludge qualification process. The measured Tank 40 composition was used in this study as the reference point for estimating the concentrations of those species not measured downstream.

The Sludge Receipt and Adjustment Tank (SRAT) is where the sludge feed is brought in, neutralized with nitric acid and blended with input streams from the Modular CSSX Unit (MCU) and Actinide Removal Process (ARP). The pH of the SRAT content is further reduced by adding formic acid, which acts as a reducing agent for HgO and MnO_2, and the content is boiled under total reflux for an extended period of time to steam strip Hg. The nitrite is also destroyed during the boilup. The resulting SRAT product is analyzed for the elemental, anions, total organic carbon (TOC), total inorganic carbon (TIC), total U and Th, and Cs-137 but no other radioisotopes. The analytical results of the SRAT product were used to cross-check the charge-reconciliation results of the Slurry Mix Evaporator (SME) product composition.

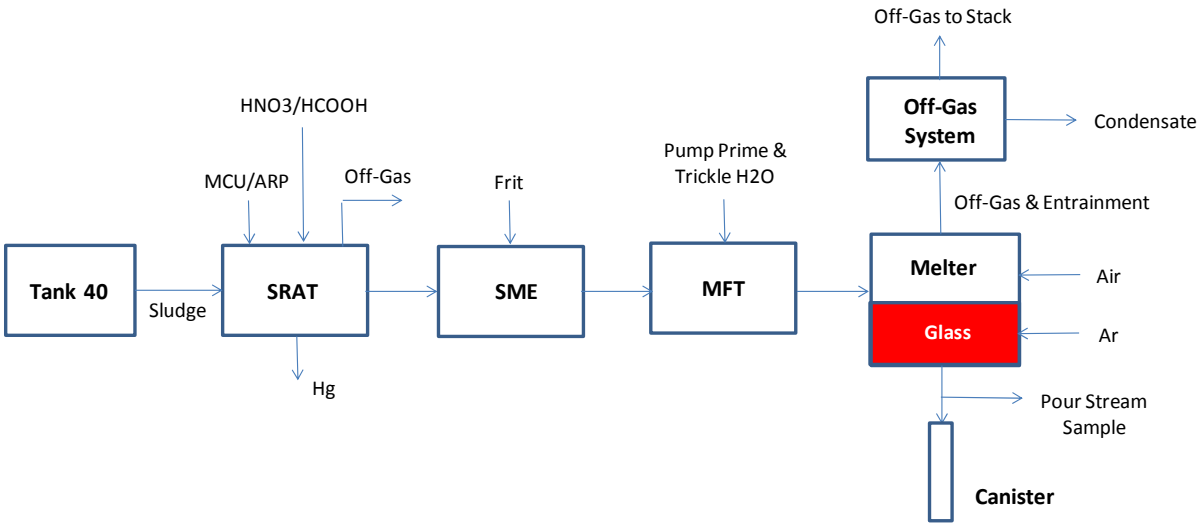

Figure 1. Simplified DWPF Process Flow Diagram.

The SRAT product is transferred to the SME in a ~4,500 gallon batch, blended with the glass forming frit and the content is boiled down to a target level. The remaining SME content is sampled and analyzed for elemental, anions, total organic carbon (TOC), total U and Th, and Cs-137 but no other radioisotopes. Once the Technical Safety Requirement (TSR) limits are met, the SME product is transferred to the Melter Feed Tank (MFT). While being fed to the melter, the MFT content is continually diluted every time the transfer pump is started up and by a constant trickle flow of water. The MFT content is sampled at every 5th batch and analyzed for the pH, density and total solids only. Since no chemical reactions are expected to occur in the MFT, the compositions of the SME product and MFT content in principle should be the same on a dry basis, ignoring the effect of tank heel. As a result, the analytical results of each SME product were used in this study to develop the composition of the corresponding MFT batch, which was adjusted further to account for the dilution by water addition prior to being fed to the melter.

3.0 Assumptions of Mixing Model

The proposed method of estimating off-gas entrainment rates as the difference between the calcined feed and glass pour rates of individual species (or the sum of all species for the overall entrainment rate) is based on the following assumptions:

1. The feeding and pouring operation over one canister-filling cycle is steady state.

2. The glass (melt) level remains constant.

3. The mixing in the glass (melt) pool is perfect.

The duration of each canister filling cycle is typically ~21 hours. Although the measured feed rate is likely to remain relatively constant during that time, the instantaneous glass pour rate fluctuates more especially near the end of a filling cycle. Assumption #1 enables use of the time-averaged feed/pour rates in the mass balance calculations. A constant glass level (Assumption #2) requires that the volumetric flow rate of calcined solids entering the glass pool (from the cold cap) equal that of the glass being poured, which in essence means that off-gas entrainment is zero. However, as long as the overall entrainment rate

is not large (e.g., < ~5% fed), the measured glass level should remain relatively constant. Since the DWPF melter has a large melt surface area (28.3 ft^2), even a small change in glass level before and after the pour could translate into a significant mass of glass over- or under-accounted for in the estimation of steady state pour rate, and this assumption helps the estimated pour rate be in line with the measured calcine feed rate. For example, if there was a net decrease of 1 inch in glass level, the measured pour rate must be adjusted down by ~17 lb/hr (= 350 lb glass/inch * 1 in / 21 hr), which is equivalent to ~9% of the nominal pour rate. Likewise, if there was a net increase in glass level, the measured pour rate must be adjusted up by the amount of glass above the initial glass level. The net level changes before and after the pour are typically small, i.e., on the order of 1-2% of the nominal glass of level of 32.7".

Ideal mixing (Assumption #3) simplifies the calculation of the varying melt composition upon feeding successive MFT batches. One drawback is that the calcined/fused solids exiting the cold cap is assumed to blend into the melt pool instantly, which is not feasible considering the high viscosity of glass melt, which is three orders of magnitude or higher than that of water. To overcome this difficulty, a full glass residence time in the melt pool was subtracted in the calculation of melter turnover by the last batch,[5] which may be excessive under the forced-convection mixing induced by the glass bubblers. The mixing delay is further examined in this study.

4.0 Mass Balance Analysis

In actual melter operation, the composition of glass being poured could be quite different from that of the calcined feed being fed at the same time for two main reasons. First, the feed composition can change appreciably from one MFT batch to the next even though the sludge feed originates from the same Tank 40 batch due to the timing and varying volumes of the MCU/ARP additions and the inhomogeneity in tank mixing, etc. Second, even under the perfect-mixing scenario, it would take 4 to 5 melter turnovers to flush out over 99% of a given batch of feed. One melter turnover is defined as when the cumulative volume of calcined solids fed equals one melt pool volume. At the nominal melt level of 32.7", the DWPF melter contains over 12,000 lb of glass, which is enough to fill three canisters, and the nominal glass residence time is on the order of 50-60 hours. Thus, in order to calculate off-gas entrainment rates of individual elements as the difference between the feed and pour rates of a particular element, it is essential to know the composition of the "composite" feed spanning several MFT batches that is representative of the melt pool composition at the time of glass PS sampling but without entrainment. For that, a mixing model is required that accounts for the effects of melt pool volume (or holdup) and residence time as well as the incoming batch volume and composition on the glass composition.

4.1 Mixing Model

The derivation of the mixing model for the estimation of glass composition after successive multiple MFT batch feeding was given earlier and will not be repeated here.[5] It was shown that the concentration of species *i* in glass at the end of n^{th} MFT batch feeding, $\boldsymbol{x_{g,i}(t_n)}$, is calculated from Eq. (1):

$$x_{g,i}(t_n) = x_i(n) + \left[x_{g,i}(t_{n-1}) - x_i(n)\right] \exp[-N_n] \quad (1)$$

where $x_{g,i}(t_{n-1})$ = concentration of species *i* in glass at the end of $(n\text{-}1)^{th}$ MFT batch feeding, lb/lb
$x_i(n)$ = measured concentration of species *i* in n^{th} MFT batch, lb/lb calcine solids
N_n = # of melter turnovers during n^{th} MFT batch feeding

The rate of off-gas entrainment of species *i*, $\dot{m}_{e,i}$, is calculated from Eq. (2):

$$\dot{m}_{e,i} = \dot{m}_{cs}(n)\, x_{g,i}(t_n) - \dot{m}_g(k)\, x_{ps,i}(k) \quad (2)$$

where k = canister # being filled while the PS sample was taken.
$\dot{m}_{cs}(n)$ = average feed rate of n^{th} MFT batch during k^{th} canister filling, lb calcine solids/hr
$\dot{m}_{g}(k)$ = average glass pour rate during k^{th} canister filling, lb/hr
$x_{ps,i}(k)$ = measured concentration of species i in PS sample, lb/lb.

4.2 Case Study: SB7a

The PS sample for the SB7a was taken on 8/5/2011 at 14:20 hour while Canister #3619 was being filled and MFT batch 580 (MFT580) had been fed for ~65 hours. The glass pool was agitated with four bubblers at the total argon (Ar) flow rate of 5.6 scfm. The operating history and feed property data for MFT580 and four preceding batches, MFT576-579 are summarized in Table 1. The total processing time for the five MFT batches was ~540 hours and the melter was left idling for a total of < 19 hours or 3.4% of the time. The total glass poured was 96,500 lb, which is equivalent to ~25 filled canisters. Particularly, during the processing of MFT576-579, enough glass had been poured to achieve 6.2 melter turnovers and, based on the ideal mixing assumption, 99.8% of the glass remaining at the end of MFT575 would have been flushed out of the melter by the time MFT580 feeding began (see Figure 3, Ref. 5). Thus, using the MFT576 calcine solid composition as the starting glass pool composition would be a good approximation for predicting the glass pool composition at the time of SB7a PS sampling using Eq. (1). The total solids and density data given in Table 1 are shown to decrease from the beginning to the end of each MFT batch as the MFT content was constantly diluted by the addition of pump prime and trickle water flows.

4.2.1 Mass Balance Equations of SB7a

Eq. (1) was applied for each successive MFT batch using MFT576 as the starting melt pool composition as follows:

$$MFT577: \quad x_{g,i}(577) = x_i(577) + \left[x_{g,i}(576) - x_i(577)\right]\exp[-N_{577}] \tag{3}$$

$$MFT578: \quad x_{g,i}(578) = x_i(578) + \left[x_{g,i}(577) - x_i(578)\right]\exp[-N_{578}] \tag{4}$$

$$MFT579: \quad x_{g,i}(579) = x_i(579) + \left[x_{g,i}(578) - x_i(579)\right]\exp[-N_{579}] \tag{5}$$

$$MFT580: \quad x_{g,i}(580) = x_i(580) + \left[x_{g,i}(579) - x_i(580)\right]\exp[-N_{580}] \tag{6}$$

where $x_i(n)$ represents the composition of the n^{th} MFT batch on a calcined solids basis and $x_{g,i}(n)$ the melt pool composition as a result of n^{th} MFT batch feeding up to the time of PS sampling. In other words, both N_{580} and $x_{g,i}(580)$ are evaluated at the time of pour stream sampling rather than at the end of MFT580 feeding.

Finally, the rate of off-gas entrainment for species i was calculated as follows:

$$\dot{m}_{e,i} = \dot{m}_{cs}(580)\, x_{g,i}(580) - \dot{m}_{g}(3619)\, x_{ps,i}(3619) \tag{7}$$

where $\dot{m}_{cs}(580)$ and $\dot{m}_{g}(3619)$ are the time-averaged calcine solids feed and pour rates, respectively, over the duration of Canister #3619 filling cycle and $x_{ps,i}(3619)$ is the measured concentration of species i in the glass pour stream that filled Canister #3619. With the exclusion of cold cap modeling in this study, Eq. (7) was applied on an elemental basis rather than on an oxide basis.

Table 1. Operating History and MFT Batch Bulk Properties for SB7a Mass Balance [7].

Batch #	Start Feeding	Stop Feeding	Duration (hour)	Average Feed Rate (gpm)	MFT Total Solids (wt%)	MFT Density (g/ml)	Total Glass Poured (lb)	Average Pour Rate (lb/hr)
576	7/15/2011 5:47	7/15/2011 6:18	0.52		34.94	1.3016		
	7/15/2011 6:29	7/17/2011 1:18	42.82					
	7/17/2011 1:38	7/17/2011 6:00	4.37					
	7/17/2011 6:08	7/18/2011 15:36	33.47					
	7/18/2011 16:17	7/19/2011 12:09	19.87	1.031	31.61	1.2165	18,734	185.4
	Total Elapsed Time =		102.37					
577	7/19/2011 12:09	7/19/2011 19:38	7.48		34.80	1.2650		
	7/19/2011 19:54	7/20/2011 16:01	20.12					
	7/20/2011 16:15	7/21/2011 2:49	10.57					
	7/21/2011 3:04	7/21/2011 14:21	11.28					
	7/21/2011 14:29	7/23/2011 3:38	37.15					
	7/23/2011 4:00	7/24/2011 5:40	25.67					
	7/24/2011 5:58	7/24/2011 6:57	0.98	1.048	30.91	1.2432	21,015	185.6
	Total Elapsed Time =		114.80					
578	7/24/2011 6:57	7/25/2011 15:41	32.73		37.65	1.2768		
	7/25/2011 15:58	7/25/2011 18:02	2.07					
	7/25/2011 18:14	7/26/2011 14:24	20.17					
	7/26/2011 14:45	7/28/2011 12:52	46.12					
	7/28/2011 20:41	7/29/2011 10:03	13.37	1.037	34.18	1.1700	21,463	187.5
	Total Elapsed Time =		123.10					
579	7/29/2011 10:03	7/31/2011 6:14	44.18		37.94	1.2630		
	7/31/2011 6:25	8/1/2011 7:54	25.48					
	8/1/2011 8:12	8/1/2011 14:57	6.75					
	8/1/2011 15:23	8/1/2011 17:35	2.20					
	8/1/2011 17:50	8/2/2011 16:22	22.53	1.049	35.02	1.1947	18,355	181.5
	Total Elapsed Time =		102.32					
580	8/2/2011 16:22	8/4/2011 4:32	36.17		37.87	1.2620		
	8/4/2011 9:48	8/5/2011 20:14	34.43					
	8/5/2011 20:35	8/6/2011 16:50	20.25					
	8/6/2011 17:06	8/6/2011 17:30	0.40	1.049	34.09	1.2491	16,932	185.6
	Total Elapsed Time =		97.13					
Can # 3619	PS sample taken @	8/5/2011 14:20	20.82	1.032	35.15	1.2527	3,920	188.3

4.2.2 Feed Chemistry of SB7a

This section describes the bases and assumptions made to develop the compositions of MFT576 to 580, i.e., $x_i(n)$'s in Eqs. (3) to (6).

4.2.2.1 Charge Reconciliation of SME Product Data

The analytical data for the SB7a Slurry Mix Evaporator (SME) products are shown in Table 2. Charge imbalance that existed in the data was reconciled under the constraints of measured bulk properties such as pH, density and total/calcined solids as well as reported waste loading (WL). In doing so, the following bases and assumptions were applied:

- All uranium (U) was assumed to be present as insoluble $Na_2U_2O_7$.
- 80% of measured Ca and 60% of measured Mn were assumed to be soluble.
- No sulfur was reported in the Inductively Coupled Plasma Atomic Emission Spectroscopy (ICP-AES) data. As a result, the sulfur reported as SO_4 by Ion Chromatography (IC) was assumed to represent 100% of sulfur in the SME samples, i.e., no insoluble sulfate.
- The insoluble oxalate, calculated as the difference between the total and soluble oxalate (by IC), was assumed to be present as CaC_2O_4.
- All anion data by IC was taken without any adjustments.
- All elemental data by ICP-AES was taken without any adjustments except for Na.

The results of charge reconciliation are shown in Table 3. The measured Na concentrations needed to be adjusted up by 3-13%, which indicates that although the reported SME data was generally in line with the expected analytical uncertainty of ±10%, the total equivalent charge of the anions was consistently greater than that of the cations for all five SME batches. As a result, the total solids of the charge-reconciled SME products were all higher than the measured values but by less than 8%. The concentration of carbonate (CO_3) was not measured so it was back calculated as the difference between the equivalent molar cation and anion concentrations after the adjustment of Na. As expected, the concentration of total inorganic carbon (TIC) thus calculated was found to be proportional to the measured pH and also in line with those of the SRAT products at the comparable pH's. In fact, the Na adjustments made were mostly to allow carbonate to be present in the melter feed at the concentrations expected at the measured pH. For example, much of the 13% increase in Na made for SME576 was used to counterbalance ~3,000 ppm carbonate at pH = 8.6.

The percent insoluble Na, which consists mostly of frit Na and diuranate precipitate ($Na_2U_2O_7$) was also calculated as part of the charge reconciliation. As expected, SME578 has the lowest PCCS WL at 36.62% and thus the highest insoluble Na at 34%, while SME577 has the highest PCCS WL at 38.86% and thus the lowest insoluble Na at 31%. The same trend is not as readily discernable with the calculated WL's, particularly for MFT580. The antifoam carbon remaining in the SME product was calculated as the difference between the measured total organic carbon (TOC) and the sum of formate and oxalate carbons. The resulting antifoam carbon concentrations were as high as ~1,800 ppm for SME576 or SME579, which is consistent with the large antifoam additions made during the SB7a SRAT/SME processing.

Table 3 also shows that the calculated waste loadings (WL) were in good agreement with those reported in the PCCS spreadsheet except for SME580, where the calculated WL was 6.1% higher than the PCCS WL. This was because the measured concentrations of all four frit components (B, Li, Na and Si) of SME580 were below their respective target values, whereas for the other SME batches some components were above and some were below their respective target values so the net difference was either slightly negative or positive, i.e., by < ±1%. This is reflected in Table 2; despite its WL being the third lowest of the five SME batches, the concentrations of B, Li and Si of SME580 are the lowest of all. The same trend cannot be discerned as readily for Na because only ~30% of the total Na originated from frit.

Table 2. SB7a SME Product Analytical Data Used in Charge Reconciliation.

Elements:	SME576 (wt% calcine)	SME577 (wt% calcine)	SME578 (wt% calcine)	SME579 (wt% calcine)	SME580 (wt% calcine)
Al	4.85	5.18	4.82	4.80	5.30
B	1.57	1.49	1.57	1.46	1.31
Ca	0.33	0.34	0.31	0.32	0.33
Cr	0.03	0.03	0.05	0.06	0.03
Cu	0.03	0.03	0.04	0.04	0.04
Fe	6.60	6.86	6.18	5.95	6.53
K	0.01	-	0.01	0.05	0.26
Li	2.36	2.14	2.31	2.41	2.07
Mg	0.18	0.18	0.17	0.15	0.17
Mn	1.70	1.76	1.56	1.48	1.66
Na	10.28	10.57	10.73	9.91	10.62
Ni	1.07	1.08	0.97	0.95	0.99
Si	24.23	23.89	23.51	22.37	21.13
Th	0.77	0.72	0.65	0.74	0.67
Ti	0.33	0.14	0.43	0.64	0.30
U	1.92	2.00	1.83	1.94	2.18
Zr	0.11	0.12	0.11	0.10	0.12
Total	56.35	56.52	55.25	53.35	53.71
Anions:	**(mg/kg)**	**(mg/kg)**	**(mg/kg)**	**(mg/kg)**	**(mg/kg)**
NO_3	17,788	20,349	22,752	22,528	22,583
COOH	34,362	30,096	31,932	33,135	31,022
C_2O_4	2,583	2,453	2,807	2,904	2,942
SO_4	1,562	1,596	1,579	1,540	1,611
NO_2	< 501	< 540	< 543	< 529	1,473
F	< 501	< 540	< 543	< 529	< 495
Cl	< 501	< 540	< 543	< 529	< 495
PO_4	< 501	< 540	< 543	< 529	< 495
total C_2O_4	4,125	3,916	4,113	4,546	4,437
Misc.					
TOC (mg/kg)	11,231	9,758	9,987	11,279	10,418
Cs-137 (Bq/g)	1.856E+07	1.373E+07	1.077E+07	1,077E+07	2,391E+07
Density (g/ml)	1.3168	1.3293	1.3770	1.3558	1.3743
Total Solids (wt%)	40.52	40.50	44.17	42.94	41.99
Calcined Solids (wt%)	35.12	34.92	38.47	37.38	36.15
pH	8.6	9.2	8.2	7.7	9.4

Table 3. Results of Charge Reconciliation of SB7a SME Product Analytical Data.

	SME576	SME577	SME578	SME579	SME580
Measured Na (wt% calcine)	10.283	10.567	10.732	9.907	10.624
Calculated Na (wt% calcine)	11.620	11.412	11.053	10.799	11.155
% Na adjustment	13	8	3	9	5
Insoluble sodium (% total Na)	31	31	34	32	32
Measured total solids (g/L)	533.5	538.3	608.2	582.2	577.0
Calculated total solids (g/L)	571.6	573.3	648.7	626.0	620.7
Δ total solids (%)	7.1	6.5	6.7	7.5	7.6
PCCS WL (%)	37.55	38.86	36.62	37.91	37.71
Calculated WL (%)	37.92	38.82	36.98	38.28	40.01
Δ WL (%)	1.0	-0.1	1.0	1.0	6.1
Calculated TIC (mg/kg)	726	968	798	672	1,005
@ measured pH	8.6	9.2	8.2	7.7	9.4
Calculated antifoam carbon (mg/kg)	1,589	835	703	1,560	1,119
Calculated Ca as oxalate (% total Ca)	80.3	74.1	64.2	78.2	70.0

4.2.2.2 Dilution of MFT Batches

Once the SME product is transferred to the MFT, it is blended with the heel and continuously diluted with both pump prime and trickle water flows until it is fed to the melter. This means that the composition of calcine solids in each MFT batch should be the same as those of the corresponding SME batches shown in Table 2, ignoring the impact of heel composition. Furthermore, although the MFT content is no longer analyzed for the full elemental and ionic compositions, every 5th MFT batch is analyzed for total solids, density and pH. This gave an opportunity to check the estimated total solids and density at the beginning of MFT580 provided by the DWPF personnel against measured data and it was found that the estimated total solids and density were 6.6% and 1.1% higher than those measured, respectively. Assuming that the same percent errors also applied to the remaining batches, the final total solids and densities of MFT576 to MFT580 adjusted down for the mass balance calculations are shown in Table 1.

Calculated elemental compositions of MFT576 to MFT580 in weight percent (wt%) calcined solids (CS) are compared in Table 4 to the elemental compositions of Tank 40 in wt% total solids (TS) and the PS glass sample in wt% (note the slurry composition in wt% CS is the same as wt% in glass).[6,8,9] As stated above, these MFT batch compositions represent $x_i(n)$ in Eqs. (3) to (6). The SME product analysis was limited in scope compared to Tank 40; some of the minor species including the noble metals were not measured, and Cs-137 was the only isotope measured. As a result, those MFT concentrations in blue text, including Tc-99, were estimated by iteration until the calculated ratios to Fe matched their respective ratios in Tank 40. This is a reasonable approximation since they are neither added nor removed during the SRAT/SME processing. Those species whose measured concentrations in Tank 40 were below detection levels are denoted by a hyphen and their corresponding concentrations in the SME or MFT are left blank since their Fe ratios in Tank 40 were not available. As expected, the concentrations of the main sludge components such as Al, Fe, Mn and U decreased from those of Tank 40 on average by a factor of 2.35 (called a dilution factor) due to; (1) frit addition and, to a lesser degree, (2) the difference in composition bases used, i.e., wt% TS vs. wt% CS. The concentrations of Ti and Cs-137 in the MFT increased due to the inputs from the Actinides Removal Process (ARP) and the Modular CSSX Unit (MCU), respectively.

Table 4. Comparison of SB7a MFT Batch Compositions to Tank 40 and PS Sample [Ref. 6,8,9].

Element	Tank 40	MFT576	MFT577	MFT578	MFT579	MFT580	PS Glass	
	(wt% TS)	(wt% CS)	(wt% CS)	(wt% CS)	(wt% CS)	(wt% CS)	(wt%)	Method*
Al	10	4.85	5.18	4.82	4.80	5.30	4.54	PF
B	-	1.57	1.49	1.57	1.46	1.31	1.33	PF
Ba	0.1	0.05	0.05	0.04	0.04	0.05	0.04	PF
Ca	0.72	0.33	0.34	0.31	0.32	0.33	0.33	AR
Cd	0.036	0.02	0.02	0.02	0.02	0.02	0.02	PF
Ce	0.13	0.06	0.06	0.06	0.06	0.06	0.03	AR
Co	0.012	0.01	0.01	0.01	0.01	0.01	-	-
Cr	0.046	0.03	0.03	0.05	0.06	0.03	0.05	PF
Cu	0.12	0.03	0.03	0.04	0.04	0.04	0.32	PF
Fe	14	6.60	6.86	6.18	5.95	6.53	6.04	AR
Gd	0.11	0.05	0.05	0.05	0.05	0.05	0.04	PF
K	0.054	0.01	0.00	0.01	0.05	0.26	<0.06	AR
La	0.078	0.04	0.04	0.03	0.05	0.04	0.03	PF
Li	0.029	2.36	2.14	2.31	2.41	2.07	2.12	PF
Mg	0.37	0.18	0.18	0.17	0.15	0.17	0.16	PF
Mn	3.9	1.70	1.76	1.56	1.48	1.66	1.56	PF
Na	13	11.62	11.41	11.05	10.80	11.16	9.23	AR
Nd	0.23	0.11	0.11	0.10	0.10	0.11	-	-
Ni	2.4	1.07	1.08	0.97	0.95	0.99	0.96	PF
P	0.060	0.03	0.03	0.03	0.03	0.03	<0.17	PF
Pb	0.027	0.01	0.01	0.01	0.01	0.01	<0.14	PF
Pd	0.003	0.00	0.00	0.00	0.00	0.00	0.003	PF
Ag	0.02	0.01	0.01	0.01	0.01	0.01	0.01	PF
Rh	0.02	0.01	0.01	0.01	0.01	0.01	0.005	PF
Ru	0.09	0.04	0.05	0.04	0.04	0.04	0.03	PF
S	0.23	0.16	0.16	0.14	0.14	0.14	<0.15	AR
Si	1.2	24.23	23.89	23.51	22.37	21.13	21.05	AR
Sr	0.048	0.02	0.02	0.02	0.02	0.02	0.02	AR
Th	1.5	0.77	0.72	0.65	0.74	0.67	0.61	PF
Ti	0.018	0.33	0.14	0.43	0.64	0.30	0.40	PF
U	4.7	1.92	2.00	1.83	1.94	2.18	2.06	PF
Zn	0.043	0.02	0.02	0.02	0.02	0.02	0.06	AR
Zr	0.14	0.11	0.12	0.11	0.10	0.12	0.11	AR
Cs-137	6.80E-04	5.78E-04	4.28E-04	3.36E-04	3.36E-04	7.45E-04	4.93E-04	
Tc-99	6.10E-04	2.87E-04	2.99E-04	2.69E-04	2.59E-04	2.85E-04	1.07E-04	
Total	53.434	58.31	58.02	56.16	54.82	54.85	51.158	

Hg at 1.9 wt% TS in Tank 40 not shown; * Dissolution method, PF = peroxide fusion, AR = aqua regia.
The Na data in red text represents modified values during charge reconciliation, as outlined in Table 3.

4.2.3 Bases and Assumptions of Mass Balance

Table 5 lists the values of key operating parameters used to calculate the off-gas entrainment rates using Eqs. (3) to (7). Some of the key bases and assumptions discussed thus far are re-summarized as follows:

1. Available analytical results for the SB7a pour stream sample taken at 14:20 hour on 8/5/2011 provided the glass composition for the mass balance.[6]

2. The melter operating data, including the feed and pour rates, $\dot{m}_{cs}(580)$ and $\dot{m}_{g}(3619)$ in Eq. (7), respectively, were time-averaged over the duration of Canister #3619 filling cycle.

3. The number of preceding MFT batches included in the calculation of the "composite" feed composition was set at a value which would result in a sufficient number of melter turnovers to flush out 99% of the old melt pool composition under perfect mixing without off-gas entrainment.

4. The composition of MFT576 in Table 4 represented the initial melt pool composition, i.e., $x_i(576) = x_{g,i}(576)$

5. The effect of heel on the MFT batch composition is ignored.

6. The melter turnover for MFT580 was reduced by the calcination time of 2 hours.

7. The measured average feed rate (FIC3309) of 1.032 GPM during the Canister #3619 filling cycle was reduced by 7.5%.

Table 5. Operating Parameters and MFT580 Properties for SB7a Mass Balance Calculations.

Parameters	Value
Melter turnover:	
- N_{576}	1.26
- N_{577}	1.41
- N_{578}	1.52
- N_{579}	1.38
- N_{580}	0.94
Mass flow rate:	
- $\dot{m}_{cs}(580)$ (lb/hr)	187.81
- $\dot{m}_{g}(3619)$ (lb/hr)	179.73
Can #3619 filling cycle (hr)	20.82
MFT580:	
- density (g/ml)	1.2527
- total solids (wt%)	36.27
- calcination time (hr)	2.00
- glass density (g/ml)[6]	2.69

Assumption #7 was based on the observation that the measured slurry feed rates tend to be higher than those estimated based on actual tank level changes by up to 15%.[7] In this study, the error margin was set at 50% of the maximum value. It is also noted that the average glass pour rate of 188.3 lb/hr during the Canister #3619 filling (Table 1) was adjusted down to 179.73 lb/hr since there was a net melt level drop of 0.51" after the filling was complete.

Melter turnovers (N) were calculated by dividing the total mass of calcined solids fed for a given MFT batch by the mass of glass in the melt pool. For example, N_{580} was calculated first by estimating the total MFT580 calcined solids fed up to the time of PS sampling, $m_{CS,580-}$ as:

$$\left(1.049\,\frac{gal}{min}\right)(0.925)\left(60\,\frac{min}{hr}\right)(64.7-2.0\ hr)\left(3785.4\,\frac{ml}{gal}\right)\left(\frac{1.2620+1.2527}{2}\,\frac{g}{ml}\right)\left(\frac{1}{453.6}\,\frac{lb}{g}\right)$$

$$\left(\frac{0.3787+0.3515}{2}\,\frac{lb_{solid}}{lb}\right)\left(0.861\,\frac{lb_{cs}}{lb_{solid}}\right) = 12{,}037\ lb_{cs}$$

where 1.049 gal/min = average feed rate of MFT580 up to the PS sampling (as indicated by FIC3309),
0.925 = correction factor for FIC3309 (Assumption #7),
64.7 hr = cumulative MFT580 feeding time up to the PS sampling (calculated from Table 1),
2.0 hr = process delay time in converting feed solids to glass (applies only to the last batch),
1.2620 g/ml = initial density of MFT580 (Table 1),
1.2527 g/ml = density of MFT580 at the time of PS sampling (Table 1),
0.3787 lb_{solid}/lb = initial total solids content of MFT580 (Table 1),
0.3515 lb_{solid}/lb = total solids content of MFT580 at the time of PS sampling (Table 1),
0.861 lb_{cs}/lb_{solid} = calcined-to-total solids ratio of MFT580, called calcination ratio (Table 2).

The melter turnover by MFT580 (N_{580}) is then calculated by dividing the total mass of MFT580 calcined solids fed, $m_{CS,580-}$, by the mass of glass that the DWPF melter holds, which is estimated to be 12,825 lb based on the melt pool volume of 76.37 ft^3 and the measured glass density of 2.69 g/ml:[6]

$$N_{580} = (12{,}037\ lb_{cs})/(12{,}825\ lb_{glass}) = 0.94$$

4.2.4 Calculation Steps

The mass balance calculations proceeded as follows:

1. Set $x_{g,i}(576)$ = concentration of species *i* in the "MFT576" column of Table 4.
2. Set $x_i(577)$ = concentration of species *i* in the "MFT577" column of Table 4.
3. Substitute $x_{g,i}(576)$ and $x_i(577)$ along with N_{577} from Table 5 into Eq. (3) and solve for $x_{g,i}(577)$.
4. Set $x_i(578)$ = concentration of species *i* in the "MFT578" column of Table 4.
5. Substitute $x_{g,i}(577)$ and $x_i(578)$ along with N_{578} from Table 5 into Eq. (4) and solve for $x_{g,i}(578)$.
6. Repeat Steps 4 and 5 for MFT579 and MFT580 and solve for $x_{g,i}(580)$.
7. Set $x_{ps,i}(3619)$ = concentration of species *i* in the "PS Glass" column of Table 4.
8. Substitute $x_{g,i}(580)$, $x_{ps,i}(3619)$ and the calcined feed and glass pour rates, $\dot{m}_{cs}(580)$ and $\dot{m}_g(3619)$ from Table 5, into Eq. (7) and calculate the off-gas entrainment rate of species *i*, $\dot{m}_{e,i}$.

4.3 Results of SB7a Mass Balance

The elemental and isotopic mass balance results of SB7a are shown in Table 6 and Table 7, respectively. It is noted that the composite MFT concentrations given in wt% CS represent $x_{g,i}(580)$ in Eq. (6) and Eq. (7), and they were calculated using the mixing model by taking into account four preceding MFT batches. The concentrations of those MFT constituents in blue text were not measured during the SME product analysis so they were estimated by fixing the concentration ratios with respect to Fe at their respective values in Tank 40.[8,9] It is noted that because Reference 8 reports only those constituents at concentrations ≥ 0.1 wt% TS, the original archived data sheets were used to retrieve data for those constituents at < 0.1 wt% TS such as Cd and Sr. The concentrations of noble metals in Tank 40 were taken from the compiled data set for the SB4 to SB7b WAPS samples.[10] Because Cs-137 was the only radionuclide analyzed for the SME samples (besides the total U and Th), the concentrations of the remaining isotopes in the MFT were estimated at their respective ratios to Fe in Tank 40. The resulting MFT concentrations are shown to sum up to 100.0% on an oxide basis, which gives credence to the SME product analytical data used in the charge reconciliation and the method used to estimate the concentrations of those minor constituents not measured using their respective ratios to Fe in Tank 40. The analytical results of the SME samples came from the DWPF Analytical Laboratory.

However, the analytical results of the PS samples do not appear to be as consistent as those of the SME samples as the former sum up only to 93.0% on an oxide basis.[6] The PS samples were analyzed in the Shielded Cells by the Analytical Development of SRNL. As a result, the measured concentrations of all PS constituents were increased uniformly by 7.5% so that the calculated glass pour rate would equal the measured average rate of 179.73 lb/hr in Table 5. The off-gas entrainment rate of each constituent was calculated as the difference between their individual feed and pour rates using Eq. (7), and the total net entrainment rate was calculated to be 3.837 lb/hr or 6.977 lb/hr on an oxide basis; the latter is equivalent to an overall entrainment rate of 3.7%. Although the overall entrainment rate was not calculated by explicitly including all radionuclides, it is still representative of the entire sample as the concentrations of all isotopes of U and Th in the composite MFT and PS samples sum up to ~99% of the total radionuclides measured in each stream (Table 7), and the total U and Th were already included in the calculation of the overall entrainment rate (Table 6).

Individually, the most abundant constituent, Si, had the entrainment rate of 0.6% fed, while the other two frit constituents, B and Li, had similar rates at 1.0% and 0.8%, respectively. However, the 2nd most abundant Na, ~32% of which is frit, had a much higher rate at 14.2% fed. The entrainment rates of the 3rd and 4th most abundant Fe and Al were also high at 2.2% and 8.8% fed, respectively. Of the 10 most abundant constituents (Al, B, Fe, Li, Mn, Na, Ni, Si, Th, U), which together make up ~97% of the total, U and Ni had negative entrainment rates of -0.9% and -1.5%, respectively. The implications and potential causes for the high or negative entrainment rates of some constituents are discussed next.

Table 6. SB7a Elemental Mass Flows of Composite Feed, Pour Stream and Off-Gas Entrainment.

Element	Tank 40	Composite MFT		SB7a Pour Stream		Off-Gas Entrainment	
	(wt% TS)	(wt% CS)	(lb/hr)	(wt%)	(lb/hr)	(lb/hr)	(% fed)
Al	10	5.115	9.626	4.545	8.782	0.844	8.8
B	<0.015	1.377	2.592	1.328	2.565	0.027	1.0
Ba	0.1	0.045	0.085	0.043	0.084	0.002	2.1
Ca	0.72	0.322	0.606	0.326	0.630	-0.024	-4.0
Cd	0.036	0.016	0.031	0.015	0.030	0.001	3.8
Ce	0.13	0.059	0.111	0.027	0.053	0.058	52.2
Cr	0.046	0.036	0.068	0.049	0.094	-0.026	-38.7
Cu	0.12	0.038	0.072	0.318	0.614	-0.542	-753.9
Fe	14	6.343	11.937	6.040	11.671	0.266	2.2
Gd	0.11	0.050	0.094	0.043	0.083	0.011	11.9
K	0.054	0.169	0.319	<0.061	<0.117	-	-
La	0.078	0.035	0.066	0.035	0.068	-0.001	-1.9
Li	0.029	2.191	4.123	2.118	4.092	0.032	0.8
Mg	0.37	0.163	0.306	0.163	0.314	-0.008	-2.6
Mn	3.9	1.604	3.018	1.560	3.014	0.004	0.1
Na	13	11.054	20.802	9.233	17.839	2.963	14.2
Ni	2.4	0.979	1.843	0.962	1.858	-0.016	-0.9
Nd	0.23	0.104	0.196	-	-	-	-
P	0.060	0.027	0.051	<0.173	<0.333	-	-
Pb	0.027	0.012	0.023	<0.141	<0.271	-	-
Pd	0.0026	0.001	0.002	0.003	0.006	-0.004	-160.5
Ag	0.018	0.008	0.015	0.010	0.019	-0.004	-25.9
Rh	0.019	0.009	0.017	0.005	0.010	0.007	41.3
Ru	0.094	0.043	0.080	0.030	0.058	0.022	27.8
S	0.23	0.142	0.267	<0.149	<0.288	-	-
Si	1.2	21.742	40.915	21.05	40.673	0.242	0.6
Sr	0.048	0.022	0.041	0.016	0.030	0.010	25.4
Th	1.5	0.688	1.294	0.610	1.179	0.115	8.9
Ti	0.018	0.410	0.772	0.395	0.764	0.008	1.0
U	4.7	2.082	3.918	2.058	3.976	-0.057	-1.5
Zn	0.043	0.019	0.036	0.064	0.123	-0.087	-240.1
Zr	0.14	0.115	0.216	0.114	0.221	-0.005	-2.1
Total	55.323	55.028	103.553	51.158	98.848	3.837	-
Total oxides	100.59	100.04	188.26	93.01	179.71	6.977	3.7%

** Values in blue text were estimated based on the ratios with respect to Fe in Tank 40.*

Table 7. SB7a Isotopic Mass Flows of Composite Feed, Pour Stream and Off-Gas Entrainment.

Isotope	Tank 40	Composite MFT		SB7a Pour Stream		Off-Gas Entrainment	
	(wt% TS)	(wt% CS)	(lb/hr)	(wt%)	(lb/hr)	(lb/hr)	(% fed)
Sr-90	1.00E-02	4.52E-03	8.51E-03	2.88E-03	5.56E-03	2.94E-03	34.6%
Zr-93	2.10E-02	9.49E-03	1.79E-02	2.16E-02	4.17E-02	-2.39E-02	-133.5%
Tc-99	6.10E-04	2.76E-04	5.19E-04	1.07E-04	2.06E-04	3.13E-04	60.2%
Cs-137	6.80E-04	5.86E-04	1.10E-03	4.93E-04	9.53E-04	1.50E-04	13.6%
Th-232	1.40E+00	6.33E-01	1.19E+00	5.89E-01	1.14E+00	5.31E-02	4.5%
U-233	1.40E-03	6.33E-04	1.19E-03	<2.46E-03	<4.74E-03	-	-
U-234	7.70E-04	3.48E-04	6.55E-04	<2.21E-03	<4.27E-03	-	-
U-235	3.00E-02	1.36E-02	2.55E-02	1.36E-02	2.63E-02	-7.56E-04	-3.0%
U-236	1.70E-03	7.69E-04	1.45E-03	<1.23E-03	<2.37E-03	-	-
U-238	4.50E+00	2.03E+00	3.83E+00	2.09E+00	4.03E+00	-2.05E-01	-5.4%
Np-237	3.10E-03	1.40E-03	2.64E-03	<2.70E-03	<5.22E-03	-2.58E-03	-97.8%
Pu-238	1.00E-03	4.52E-04	8.51E-04	4.59E-04	8.87E-04	-3.64E-05	-4.3%
Pu-239	2.00E-02	9.04E-03	1.70E-02	9.86E-03	1.90E-02	-2.03E-03	-11.9%
Pu-240	1.80E-03	8.14E-04	1.53E-03	<1.96E-03	<3.79E-03	-	-
Pu-241	5.50E-05	2.49E-05	4.68E-05	5.69E-04	1.10E-03	-1.05E-03	-2248%
Pu-242	<5.90E-04	<2.67E-04	<5.02E-04	<1.43E-03	<2.76E-03	-	-
Am-241	1.10E-03	4.97E-04	9.36E-04	4.47E-04	8.64E-04	7.16E-05	7.7%
total	6.00E+00	2.71E+00	5.10E+00	2.73E+00	5.27E+00	-1.76E-01	
total U	4.53E+00	2.05E+00	3.86E+00	2.10E+00	4.06E+00	-2.06E-01	
U+Th	5.93E+00	2.68E+00	5.05E+00	2.69E+00	5.20E+00	-1.53E-01	
U+Th (% total)	98.9%	98.9%	98.9%	98.7%	98.7%	86.7%	-3.5%

** Values in blue text were estimated based on the ratios with respect to Fe in Tank 40.*

5.0 Discussion

The calculated entrainment rates presented in Table 6 and Table 7 are discussed in detail next.

5.1 Overall Entrainment Rate

The design basis glass entrainment rate for the non-bubbled DWPF melter is 1% of the calcined feed.[11] Under bubbled conditions, melter pressure spikes are larger and more frequent than under non-bubbled conditions, as shown in Figure 2.[12] Since large melter pressure spikes induce large off-gas surges during which feed/glassy materials are lifted up and entrained in the melter exhaust, it is expected that entrainment will be greater during bubbled operation. Indeed, this was the case as the calculated overall entrainment rates of SB6 and SB7a were higher at 2.4% and 3.7% of the calcined feed, respectively.[5] However, although SB6 and SB7a were both blended with the same frit (Frit 418) and fed under bubbled conditions, the calculated entrainment rate of SB7a was 50% higher than that of SB6, which suggests that differing feed composition could have led to different entrainment rates. For example, when the sludge simulant was blended with a high-alkali frit, thus lowering the melt viscosity, measured overall entrainment rates under non-bubbled conditions were determined to be comparable to those under bubbled conditions.[4] As part of the scope for Stage 3 of the current task plan,[2] pressure spike data for different sludge batches will be examined closely and the impacts of pressure spikes and/or feed composition (or melt viscosity) on the overall entrainment rate will be quantified for the DWPF melter.

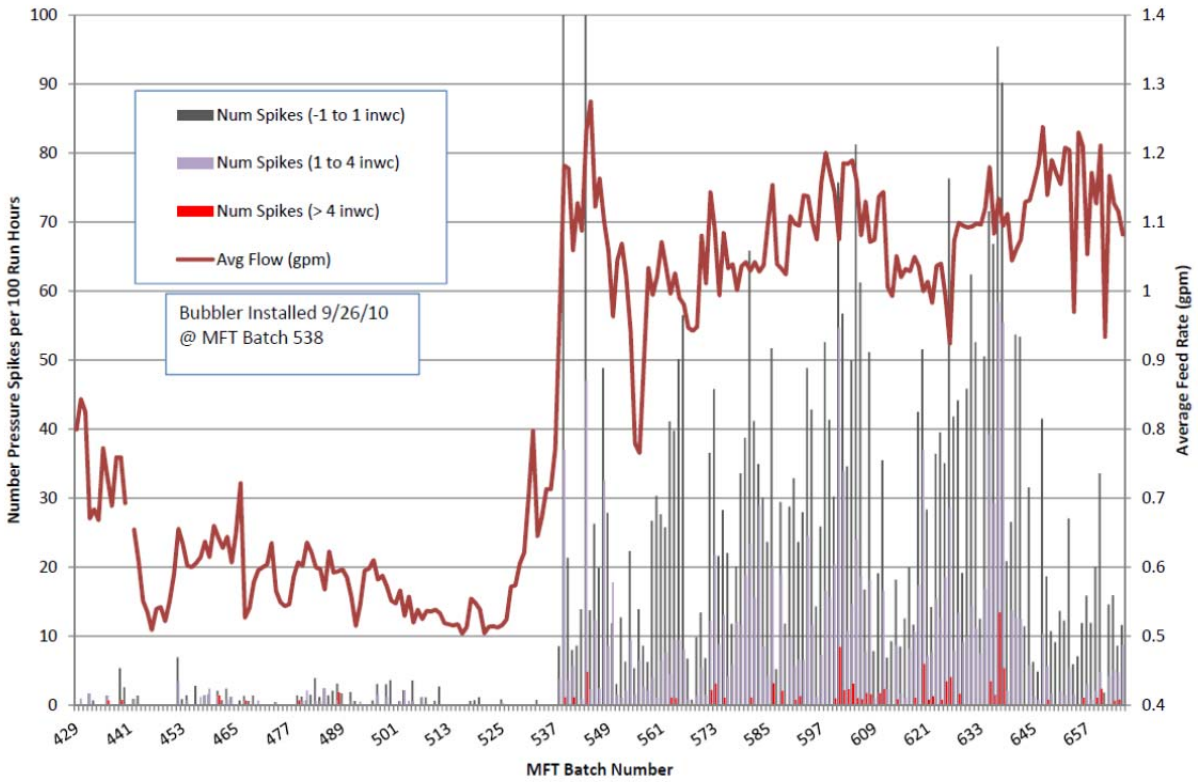

Figure 2. DWPF Melter Pressure Spikes Before and After Glass Bubbler Installation During SB6 Processing [Ref. 12].

5.2 Elemental Entrainment Rates

The higher overall entrainment rate of SB7a compared to those calculated for SB6 could also be due to the high entrainment rates of two main constituents, Al and Na, at 8.8% and 14.2%, respectively. Besides the inherent difficulties associated with the ideal melt pool mixing and steady-state assumptions, the potential sources for errors in the calculated entrainment rates include the uncertainties in the analytical results and melter operating data used. A quick comparison of the charge-reconciled individual MFT batch compositions to that of the pour stream in Table 4 offers some clues as to why the entrainment rates of Al and Na are deemed high. In principle, each MFT batch composition in Table 4 should closely represent the PS composition if the melter were fed with that particular MFT batch indefinitely, which means that the concentration of a particular constituent in the PS sample cannot be lower or higher than the lowest or highest concentration of the same constituent, respectively, in all MFT batches. However, the measured concentrations of Al and Na in the PS sample are shown to be lower than their lowest MFT counterparts, particularly for the latter, and this would clearly result in over-prediction of their respective entrainment rates. A support for this argument comes from the fact that the measured concentrations of the PS sample summed up to only 93% on an oxide basis, as shown in Table 6. In this study, however, the measured concentrations of all PS constituents were increased by the same ratio to the 100% total in lieu of increasing only those of selected species such as Al and Na since the extent to which to increase each concentration would be arbitrary.

Furthermore, according to the mixing model, the earlier the MFT batch, the less impact it would have on the PS composition, which means that the concentration of a given constituent in the PS sample is likely to lie between those in MFT579 and MFT580. Of the ten most abundant feed constituents, the reported concentration of total Th in the PS sample was also lower than its lowest MFT counterpart (MFT578) and thus its calculated entrainment rate of 8.9% appears to be high. This has been confirmed to some degree as the calculated entrainment rate of Th-232, whose mass accounts for practically 100% of all its isotopes measured in Tank 40,[10] was lower at 4.5% fed, as shown in Table 7.

The measured concentration of Si in the PS sample prepared using the aqua regia (AR) method was also slightly lower than the lowest MFT concentration in MFT580, which suggests that its entrainment rate of 0.6% fed could have been slightly over-estimated. It is noted that the calculated entrainment rate of Si for SB6 was also 0.6%.[5] When the entrainment rate of Si was calculated using the data based on the peroxide fusion (PF) method, it resulted in a negative entrainment rate of -3.9% fed, which is not consistent with the analytical results of off-gas deposit samples; Si was one of the five major species identified, including Al, Fe, Na and U.[13] So the data was rejected in favor of that based on the AR method, as noted in the last column of Table 4. Similarly, when the concentration of total Sr obtained using the PF method was used, it resulted in a negative entrainment rate of -2.5% fed, while that obtained using the AR method resulted in a positive entrainment rate of 25.4% fed, which appears to be high but is found to be comparable to that calculated for Sr-90 at 34.6% fed.

Besides Na, Si was the only major constituent whose entrainment rate was calculated using the analytical data based on the AR method. The entrainment rates of other frit constituents, B and Li, were calculated using the analytical data based on the PF method, and the resulting values were 30-70% higher than that of Si. These results were expected since both B and Li can be entrained in the off-gas not only by the physical mode but by their relative volatilities. For example, a loss of ~2% B was observed during the frit fabrication process at 1,100 °C for 30 min,[14] and the volatility of Li was confirmed by its presence in the off-gas deposit samples as alkali borate salts.[15]

Among other radioactive constituents besides Th-232 and Sr-90, the measured concentration of Cs-137 in the PS sample was between those of MFT579 and MFT580 and its calculated entrainment rate of 13.6% of the amount fed is lower than that calculated for SB6 at 16.4% but higher than the DWPF design basis

of 10% under non-bubbled conditions.[11] The estimated concentration of Tc-99 in the MFT using its ratio to Fe in Tank 40 remained relatively constant in all batches but the measured value in the PS sample was less than 50% of its lowest MFT counterpart, which suggests that the calculated entrainment rate of Tc-99 at 60.2% was likely over estimated. However, the volatility of Tc under oxidizing conditions is well known, as it could volatize as the heptoxide (Tc_2O_7), which has a boiling point of 311 °C, or sublime as an alkali metal pertechnetate, ammonium pertechnetate, or TcO_2.[16] There is no direct evidence that Tc_2O_7 is the actual volatile species, and this is because the characterization of volatile Tc species is indirect; it is based on examining the condensed product, in which Tc_2O_7 can disproportionate to the pertechnetate. Nonetheless, it does seem plausible that with its low boiling point the heptoxide could contribute to the volatile losses. Alkali pertechnetates such as $KTcO_4$ and $CsTcO_4$ are also likely to be volatile,[17] and the latter would cause a synergistic loss of Cs-137 and Tc-99 from the melter. Some studies indicate a synergistic behavior with potassium, but indications are mixed on whether the Cs and Tc losses are synergistic.[18,19] The actual volatile species may initially be $CsTcO_4$, which then dissociates to Tc_2O_7 and Cs_2O, since the latter is relatively volatile at the melt temperature.[17,19]

Furthermore, after accounting for the fraction of non-radioactive cesium in the waste, which is estimated to be ~77%,[20] the calculated entrainment rates of technetium and cesium are nearly equimolar at 1.4E-3 and 2.1E-3 mole/hour, respectively. Although an interesting observation, it does not prove that there is a synergistic behavior between these elements, but it does highlight that this is a key observation to monitor in future evaluations. Although it has been reported that $CsTcO_4$ is the most volatile and TcO_2 the least volatile in pure phases,[17] it is unclear how this would be influenced by the complex matrix of glass in DWPF or its REDOX condition. It is not known what the chemical form of Tc is in the feed to DWPF, as it could be pertechnetate ion in interstitial water or trapped in sludge particles, or could be TcO_2. Further experimental work would be needed to determine the actual volatile species and contributors to volatility.

The negative entrainment rates (shown in red text) indicate that more material was measured in the pour stream sample than was predicted by the mass balance. In some cases, the method of matching the ratios to Fe in Tank 40 to estimate the corresponding concentrations in the MFT did not yield meaningful results particularly for those minor or trace-level constituents because of their high sensitivity to the variations in the input data. In other cases, it appears that the glass sample contained metals leached out of the melter refractory or contamination during laboratory procedures. For example, Cu and Zn have large negative entrainment rates at 754% and 269%, respectively, due to the combination of being present in the MFT at <0.05 wt% (on a calcine basis) and their concentrations in the glass sample increasing nearly by an order of magnitude. In the preparation for analysis, the glass is ground using a silicon carbide grinder and then sieved. The sieves are made of brass wire, and evidently some of the brass could be abraded onto the glass particles and appear as Cu and Zn in the final analysis.

The two most dominant sludge constituents besides Na are Al and Fe, and they were expected to exhibit a similar entrainment behavior. This appears to be the case considering that the likely entrainment rate of Al would be considerably lower than 8.8%, while that of Fe was estimated to be 2.2% fed. However, even under bubbled conditions, the projected entrainment rates on the order of 2-3% for Al and Fe still appear to be high. As a comparison, the calculated entrainment rate of Fe for SB6 was 0.7%, while that of Al was 3.5X higher at 3.3% fed despite the fact that its concentration was lower than Fe by more than 20%.[5] It was postulated that the higher entrainment rate of Al under bubbled conditions could be due to aluminum leaching out of the K3 refractory (which contains alumina nominally at 60 wt%),[5] which seems plausible considering that the current DWPF Melter #2 has been in operation for over 14 years, well past its 2-year design life. However, this scenario would increase not only the entrainment but the pour rates, which could even lead to negative entrainment rates. It would be interesting to see how the calculated entrainment rate of Al would change as the method is applied to the earlier sludge batches when the Melter #2 was relatively new and before the glass bubblers were installed.

The leaching from melter components appears to be the case for Cr as its calculated entrainment ratio was -39% of the amount fed. First, its concentration in the MFT was lower than either Al or Fe by more than two orders of magnitude so even a slight change in the MFT analytical data or metal leaching/corrosion rates could have had a very large impact on its calculated entrainment rate. Second, chromium is a major constituent of both K-3 refractory (27 wt% as Cr_2O_3) and Inconel 690™ electrodes (27-31 wt%). Thus, considering the age of the current DWPF melter, additional Cr could have entered the glass pool from the leaching of either K-3 or Inconel 690™, more likely from the latter unless chromium could selectively leach out of K-3. Nickel also showed a negative entrainment ratio of -0.9% of the amount fed. However, since its concentration in the feed was 27X higher than that of Cr, its calculated entrainment ratio should have been less sensitive to the variations in analytical data or leaching/corrosion rates. Thus, the fact that ~60 wt% of Inconel 690™ is made up of Ni suggests that the negative entrainment rate of Ni may have been due to leaching of Inconel 690™. This scenario is likely if the electrodes are in or near the path of rising Ar bubbles, as demonstrated in a recent melter study using a coupon inserted into the melt pool directly in the path of Ar bubbles.[14] The fact that the calculated entrainment rate of Ni was negative for SB6 and continued to be negative for SB7a adds credence to the postulation of leaching of Inconel 690™ electrodes. This needs to be confirmed when the calculations are repeated in a future study using the data taken during non-bubbled operation.

It is further noted that despite its known relative volatility, the calculated entrainment rate of Cd was only 3.8% of the amount fed compared to 18.2% estimated earlier for SB6.[5] Since the measured concentration of sulfur in the pour stream was below the detection limit, its entrainment rate could not be calculated.

5.3 Comparison to Other Melter Data

In order to find out how the calculated entrainment rates in this study compare to other melter data, one of the melter emission studies performed at the Vitreous State Laboratory (VSL) was used as the basis. In particular, the data taken from their largest pilot melter DM1200 was used since off-gas entrainment is strongly scale-dependent with all other conditions being equal. In one such run,[3] the HLW AZ-101 simulants were fed along with the glass-forming chemicals (in lieu of frit) under different bubbler configurations. In Table 8, the calculated elemental entrainment rates of SB6 and SB7a are compared to those measured at two different bubbling rates in DM1200.

A clear trend in the bubbling rate vs. entrainment is shown in the DM1200 data; when the bubbling rate was doubled, the measured entrainment rates were also doubled more or less for all species. The general trend of increasing entrainment with increasing bubbling rate or, more accurately, increasing bubbling flux (defined as the volumetric bubbling rate per unit melt surface area) was expected since particulates would get airborne more easily at a higher linear velocity of bubbling medium. The support for this postulation comes from the same DM1200 data;[3] when the number of bubblers was doubled to four at the same total bubbling rate thereby reducing the linear bubbling velocity by half, the measured entrainment rates decreased for all species as a result.

A direct comparison between the DWPF and DM1200 entrainment rates is not straightforward and thus is not guaranteed to produce meaningful conclusions because off-gas entrainment is impacted by a host of other variables besides the bubbling flux, such as the feed chemistry and melter design characteristics. For example, when the SB6 simulants treated with three different reductants, including formic acid, glycolic acid and sugar, were fed to the DM10 melter, the resulting off-gas from the formic acid-treated feed was found to fluctuate more frequently with greater amplitude than the other feeds.[21] Fluctuating off-gas flow is an indication of off-gas surging, which provides the driving force for the entrainment of non-volatiles.

Table 8. Comparison of DWPF vs. DM1200 Melter Off-Gas Entrainment Ratios.

Melter	DWPF		DM1200	
Melt Surface Area (ft^2)	28.3		12.9	
# of Bubblers	4[1]		2[2]	
Bubbling Medium	Ar		Air	
Bubbling Rate (scfm)	5.2		2.3	4.7
Bubbling Flux (scfm/ft^2)	0.18		0.18	0.36
Reductant	Formic Acid		Sugar	Sugar
Feed	SB6	SB7a	AZ-101 simulant	
Element	(% Fed)	(% Fed)	(% Fed)	(% Fed)
Al	3.3	<8.8	0.44	0.81
B	1.9	1.0	0.90	2.03
Ba	-27.6	2.1	0.64	1.38
Ca	-9.5	-4.0	1.08	1.59
Cd	18.2	3.8	2.32	2.68
Cs-137	16.4	13.6	-	-
Cu	-628.2	-754	0.60	1.04
F	-	-	81.58[3]	35.50
Fe	0.7	2.2	0.93	1.91
K	46.2	-	5.21	5.68
Li	0.9	0.8	0.44	0.75
Mg	0.2	-2.6	1.88	3.23
Mn	5.6	0.1	0.32	0.66
Na	7.5	<14.2	1.02	1.88
Ni	-5.6	-0.9	0.58	1.08
Pb	-36.9	-	1.10	2.00
Ru	-25.4	27.8	4.08	6.18
S	> 49.2	-	40.39	46.33
Si	0.6	0.6	0.35	0.52
Sr	-8.1	-2.5	1.03	2.29
Sr-90	-	34.6		
Tc-99	-	<60.2		
Th	4.2	8.9	-	-
Th-232	-	4.5	-	-
Ti	15.0	1.0	-	-
Am-241	-	7.7	-	-
U	4.8	-1.5	-	-
Zn	-160.4	-269	0.93	1.62
Zr	31.2	-2.1	0.36	0.64
Overall	2.4	3.7	0.62[4]	1.11[4]

[1] Each with one outlet; [2] Each with two outlets; [3] From water dissolution of filter particulate;
[4] Based on gravimetric analysis of filters and rinses

If the calculated entrainment ratios of the DWPF melter are compared to those of DM1200 at the same bubbling flux of 0.18 scfm/ft^2 solely based on the reductants used, the former are indeed seen to be in general higher than the latter but by a large-than-expected margin for the major components. And it does not seem plausible that use of formic acid was the main reason for such a large margin. In fact, focusing only on the major components, the calculated DWPF entrainment ratios of Al, Mn, and U appear to be high, while those of B, Fe, and Si are quite comparable to their respective values in DM1200. On the other hand, the much higher calculated DWPF entrainment ratios of Na and semi-volatiles such as Cd and Cs than their DM1200 counterparts could be reflective of the actual melter conditions leading up to the SB7a pour stream sampling such as extended idling and/or perhaps more frequent and larger-magnitude off-gas surges. In a future study, the calculated entrainment rates of individual species will need to be interpreted by tracking the melter operating history more closely.

6.0 Conclusions

The work performed during this study remains preliminary in nature since its goal was to continue to demonstrate the feasibility of estimating the off-gas entrainment rates from the DWPF melter based on the overall as well as elemental mass balances using measured SME product and glass pour stream compositions and time-averaged melter operating variables over the duration of one canister filling cycle. The first case study performed earlier involved the SB6 pour stream sample.[5] In this work, a second case study was performed involving the SB7a pour stream sample collected on 8/5/2011 at 14:20 hour while Canister #3619 was being filled under bubbled conditions using argon. Based on the results presented and subsequent discussions given in this report, it is concluded that:

1. The proposed method of estimating off-gas entrainment rates from measured feed and pour stream compositions appears feasible and thus additional case studies are warranted. However, success of this approach requires that the analytical data for the feed and pour stream samples carry a high degree of QA pedigree and all required melter operating data be collected, analyzed, interpreted and applied correctly.

2. The overall entrainment rate from the bubbled DWPF melter was calculated to be 3.7% of the calcined solids fed, which is more than 3X the design basis entrainment rate for the non-bubbled melter. However, the analysis indicated that the result was skewed higher due to likely analytical under prediction of Al and Na contents in the pour stream sample.

3. The average entrainment rate of the four major non-volatile sludge components, including Al, Fe, Mn and U, was calculated to be 2.4% of the amount fed, while that of the frit components, excluding Na, was 0.8%. The higher entrainment rate of sludge over that of frit by a ratio of 3:1 is close to the ratio obtained earlier for SB6 and in qualitative agreement with the analytical results of two off-gas deposit samples taken at the inlet of the Quencher.

4. The 3:1 sludge-to-frit entrainment ratio determined in this study for a bubbled melter is ~1/2 that of the non-bubbled melter, which suggests that the frit components may become more prone to entrainment when the bubblers are in use.

5. The calculated entrainment rates of Cs-137 and Tc-99 were 13.6% and <60.2% of the amount fed, respectively, while that of sulfur could not be estimated due to the measured concentration of sulfur in glass was below detection level.

6. The calculated DWPF entrainment rates of B, Fe, and Si were comparable to their respective measured values during a DM1200 run. For most of the remaining species, the calculated DWPF entrainment rates were in general higher than those measured from the DM1200, which may be

attributed in part to the use of formic acid as the baseline reductant for the DWPF feeds compared to sugar used for the DM1200 feeds. On the other hand, the much higher calculated DWPF entrainment rates of Na and semi-volatiles could be reflective of actual melter conditions such as extended idling and frequent and/or larger off-gas surges.

7.0 Future Work

The proposed mass balance approach will be tested further using additional pour stream data taken under different conditions (e.g., non-bubbled operation and varying feed compositions) and, if necessary, will be adjusted and refined. In particular, work needs to focus on; (1) quantifying the uncertainty bounds of both analytical and key melter operating data, including the feed rate as indicated by FIC3309, and (2) better estimation of melter hold-up of various elements and process delays due to the cold cap reactions. Data permitting, work also needs to be expanded by including other isotopes besides Cs-137 and Tc-99. Future work also includes completing the remaining tasks necessary to enable incorporation of the results into the WTP flowsheet models. As stated in the Introduction, these tasks include; (1) completion of the collection and evaluation of all available DWPF sludge batch data, (2) thermodynamic modeling of the vitrification process, and (3) aqueous electrolyte modeling of the melter off-gas condensate chemistry.

8.0 Quality Assurance

The work defined herein is not waste form affecting, and thus does not need to follow QA requirements of RW-0333P. This technical report does not support any Type 1 calculation and thus need not be treated as a lifetime record.

Data entry and initial calculations were performed by F. G. Smith following the steps used in the previous study.[5] A. S. Choi performed a technical review of the initial calculations following the requirements for performing reviews of technical reports and the extent of review, as defined in Manual E7, Procedure 2.60. After consultation with DWPF personnel, A. S. Choi made adjustments to the initial calculations, including the charge-reconciliation of the SME product composition using the waste loading calculated as part of the SME acceptability testing, dilution of the MFT slurry and its impact on the slurry density and total solids, and fine-tuning of the mass balance calculations by using the adjusted FIC3309 data. The revised calculations were then reviewed by F. G. Smith according to the requirements of Manual E7, Procedure 2.60. D. L. McClane performed an independent review of the overall content of the report.

9.0 References

1. EMSP Project Test Plan, "Technetium Management – Hanford Site (FY2015)," ***TP-EMSP-0018***, ***Rev. 0***, U.S. Department of Energy, April 2015.

2. McCabe, D. J., and Choi, A. S., "Task Technical and Quality Assurance Plan for Technetium Management – Flowsheet Modeling Improvements for LAW Recycle Predictions," ***SRNL-RP-2014-01062, Revision 0***, Savannah River National Laboratory, Aiken, SC, October 2014.

3. Matlack, K. S., Weiliang, G., Bardakci, T., D'Angelo, N., Lutze, W., Callow, R. A., Brandys, M., Kot, W. K., and Pegg, I. S., "Integrated DM1200 Melter Testing of Bubbler Configurations Using HLW AZ-101 Simulants," ***VSL-04R4800-4***, ***Rev. 0***, Catholic University of America, Washington D.C., August 16, 2004.

4. Sabatino, D. M., "Sampling Data Summary for the Ninth Run of the Large Slurry Fed-Melter," ***DPST-83-1032***, Savannah River Laboratory, Aiken SC, November 22, 1983.

5. Choi, A. S., Kesterson, M. R., Johnson, F. C., and McCabe, D. M., "Preliminary Analysis of Species Partitioning in the DWPF Melter," ***SRNL-STI-2015-00279, Revision 0***, Savannah River National Laboratory, Aiken, SC, July 2015.

6. Johnson, F. C., and Pareizs, J. M., "Analysis of DWPF Sludge Batch 7a (Macrobatch 8) Pour Stream Samples," ***SRNL-STI-2012-00017, Revision 0***, Savannah River National Laboratory, Aiken, SC, May 2012.

7. Hodges, B. C., *Private Communications*, Savannah River Remediation, Aiken, SC, August 2016.

8. Reboul, S. H., and Click, D. R., "Stable Constituents in SB7a Tank 40 WAPS Sample," ***SRNL-L3100-2011-00133***, ***Rev. 0***, Savannah River National Laboratory, Aiken, SC, June 30, 2011.

9. Reboul, S. H., and DiPrete, D. P., "Reportable Radionuclides in DWPF Sludge Batch 7a (Macrobatch 8)," ***SRNL-STI-2011-00720***, ***Rev. 0***, Savannah River National Laboratory, Aiken, SC, December 2011.

10. Bannochie, C. J., "Tank 40 Final SB7b Chemical Characterization Results," ***SRNL-STI-2012-00097***, ***Rev. 1***, Savannah River National Laboratory, Aiken, SC, November 2012.

11. Basic Data Report – Defense Waste Processing Facility Sludge Plant, Savannah River Plan 200-S Area, Westinghouse Savannah River Co., Aiken, SC, 1982.

12. Coleman, J. C., *Unpublished Data*, Savannah River Remediation, Aiken, SC, June 2013.

13. Zeigler, K. E., and Bibler, N. E., "Characterization of DWPF Melter Off-gas Quencher and Steam Atomized Scrubber Deposit Samples," ***WSRC-STI-2007-00262***, ***Rev. 0***, Savannah River National Laboratory, Aiken, SC, May 2007.

14. Johnson, F. C., Choi, A. S., Miller, D. H., and Immel, D. M., "Comparison of HLW Glass Melting Rate Between Frit and Glass Forming Chemicals Using X-Ray Computed Tomography," ***SRNL-STI-2014-00562, Revision 0***, Savannah River National Laboratory, Aiken, SC, April 2015.

15. Jantzen, C. M., "Glass Melter Off-Gas System Pluggages: Cause, Significance, and Remediation (U)," ***WSRC-TR-90-205, Rev. 0***, Westinghouse Savannah River Co., Aiken, SC, March 1991.

16. Darab, J. G., and Smith, P. A., "Chemistry of Technetium and Rhenium Species during Low-Level Radioactive Waste Vitrification," ***Chem. Mater.***, ***8***, pp 1004-1021 (1996).

17. Vida, J., *The Chemical Behavior of Technetium during the Treatment of High-Level Radioactive Waste,* ***Dissertation, TH Karlsruhe***, 1989 (translation by Hewett, PNL-TR-497).

18. Lammertz, H., Merz, E., and Halaszovich, S. T., "Technetium Volatilization During HLLW Vitrification," ***Mat. Res. Soc. Symp. Proc.***, ***Vol. 44***, Materials Research Society (1995).

19. Cains, B. P. W., Yewer, K. C., and Waring, S., "Volatilization of Ruthenium, Caesium and Technetium from Nitrate Systems in Nuclear Fuel Processing and Waste Solidification," ***Radiochemica Acta, 56***, pp 99-104 **(**1992).

20. Data on mass 133 (2265 μg/L) from analysis of MCU Salt Batch 6 vs. Cs-137 by gamma scan (1.28E8 dpm/mL), ***ELN #-A4571-00084-06***, Savannah River National Laboratory, Aiken, SC, November 2015.

21. Choi, A. S., "Melter Off-Gas Flammability Assessment for DWPF Alternate Reductant Flowsheet Options," ***SRNL-STI-2011-00321***, ***Rev. 0***, Savannah River National Laboratory, Aiken, SC, July 2011.

Distribution:

J. C. Griffin, 773-A
D. E. Dooley, 773-A
A. P. Fellinger, 773-42A
C. C. Herman, 773-A
S. D. Fink, 773-A
B. J. Wiedenman, 773-42A
E. N. Hoffman, 999-W
F. M. Pennebaker, 999-W
K. M. L. Taylor-Pashow, 773-A
C. A. Nash, 773-42A
C. L. Crawford, 773-42A
D. J. McCabe, 773-42A
W. R. Wilmarth, 773-42A
T. B. Peters, 773-42A
A. S. Choi, 773-42A
D. T. Herman, 735-11A
A. D. Cozzi, 999-W
W. G. Ramsey, 999-W
Records Administration (EDWS)

K. H. Subramanian, WRPS
J. R. Vitali, WRPS
S. T. Arm, WRPS
M. G. Thien, WRPS
T. W. Crawford, WRPS
D. J. Swanberg, WRPS
S. D. Reaksecker, WRPS
T. L. Waldo, WRPS

R. Gimpel, RPP-WTP

N. M. Jaschke, DOE-ORP
D. L. Noyes, DOE-ORP
G. D. Trenchard, DOE-ORP
A. A. Kruger, DOE-ORP
W. F. Hamel, DOE-ORP
I. Wheeler, DOE-ORP
R. A. Gilbert, DOE-ORP

N. P. Machara, DOE-EM
J. A. Poppiti, DOE-EM
D. J. Koutsandreas, DOE-EM